NATIONAL ADVISORY COMMITTEE
FOR AERONAUTICS

TECHNICAL NOTE 3303

TURBULENT-HEAT-TRANSFER MEASUREMENTS AT

A MACH NUMBER OF 3.03

By Maurice J. Brevoort and Bernard Rashis

Langley Aeronautical Laboratory
Langley Field, Va.

NACA

Washington

September 1954

NATIONAL ADVISORY COMMITTEE FOR AERONAUTICS

TECHNICAL NOTE 3303

TURBULENT-HEAT-TRANSFER MEASUREMENTS AT

A MACH NUMBER OF 3.03

By Maurice J. Brevoort and Bernard Rashis

SUMMARY

Turbulent-heat-transfer measurements were obtained through use of a three-dimensional axially symmetric nozzle which consists of an inner shaped plug and an outer cylindrical sleeve. Measurements were taken along the outer sleeve and gave flat-plate results that are free from wall interference and corner effects for a Mach number of 3.03 and for a Reynolds number range of 5.6×10^6 to 6.5×10^7. The heat-transfer-coefficient results are in good agreement with theoretical analyses and the recovery-factor results are in good agreement with extrapolations of lower Reynolds number data.

INTRODUCTION

The design of supersonic aircraft and missiles requires engineering information about heat-transfer coefficients and recovery factors that extend over a wide range of Reynolds numbers. Each of the existing experimental techniques for studying heat-transfer characteristics appears limited in various ways. A test setup which utilizes a flat plate for the testing surface is subject to corner and edge effects and also shock interference if high Reynolds numbers are obtained by extending the plate.

One existing technique which avoids these effects is that of the hollow cylinder mounted centrally in the test section. However, the apparatus is subject to the tube choking at low Mach numbers and deviation from flat-plate conditions (the boundary-layer thickness approaching a sizable fraction of the cylinder radius) when the Reynolds numbers are low. In addition, there are differences in the heat-transfer characteristics for the inside and outside surfaces of the cylinders.

The purpose of this paper was to present results obtained by using a technique that would avoid the above-mentioned effects and permit simple and accurate measurements of local heat-transfer coefficients and

recovery factors over an extended range of both Reynolds and Mach numbers. The development of this technique for Mach number 3.03 and the results of preliminary heat-transfer measurements for the cooling of the surface by the airstream are the subject of this paper.

SYMBOLS

c specific heat of the sleeve material, $Btu/lb\text{-}^{o}R$

C_p specific heat of the air at constant pressure, $Btu/lb\text{-}^{o}R$

g acceleration due to gravity, ft/sec^2

h heat-transfer coefficient, $Btu/ft^2\text{-}sec\text{-}^{o}R$

k heat conductivity, $Btu/ft\text{-}sec\text{-}^{o}R$

m mass of the sleeve material, $pounds/ft^2$

Nu Nusselt number, hx/k

Pr Prandtl number, $\mu C_p g/k$

R Reynolds number, $\rho Vx/\mu$

η_r recovery factor, $\dfrac{T_{eq} - T_\infty}{T_{stag} - T_\infty}$

St Stanton number, Nu/RPr

T_{eq} effective stream air temperature at the wall, some temperature which gives a thermal potential which is independent of conductance h, ^{o}R

T_{stag} stagnation temperature, ^{o}R

T_w inside surface temperature of the sleeve, ^{o}R

T_∞ free-stream temperature, ^{o}R

V free-stream velocity, ft/sec

x   longitudinal distance along sleeve, ft

ρ free-stream density of the air, slugs/ft^3

μ dynamic viscosity coefficient, lb-sec/ft^2

dT/dt   time derivative of average wall temperature for a particular
                x-station, $^\circ$R/sec

APPARATUS AND METHOD

The apparatus consisted of a three-dimensional axially symmetric
nozzle which was directly connected to the settling chamber of a cold-air
blow-down jet. The nozzle consists of a shaped plug and an outer sleeve
of 8-inch extra-heavy seamless carbon-steel pipe which was machined inside
and outside to a wall thickness of 0.388 inch. A detailed drawing of the
apparatus is shown in figure 1. The ordinates of the plug are given in
table I. The plug was designed by using three-dimensional characteristics
(see ref. 1).

Details of the installation of the thermocouples and static-pressure
orifices are shown in figures 2 and 3. The thermocouples are located
0.060 inch from the inner surface of the sleeve. The wires are number-
30-gage copper-constantan (0.010 inch in diameter). For these wires,
conduction along the wire length is negligible. As indicated in figure 2,
the thermocouples are in intimate contact with the steel wall so that
thermal resistance at this junction is negligible.

Figure 1 shows the location of the static-pressure orifices. The
Mach number distribution was measured both lengthwise and around the
sleeve. The results are shown in figure 4.

The temperature-recording equipment consisted of three synchronized
high-speed Brown recorders, having a total of 36 switches, two of which
were connected to the settling-chamber thermocouples, the rest being con-
nected to the sleeve thermocouples. The stagnation-temperature variation
with time for a settling-chamber pressure of 220 pounds per square inch
gage is shown in figure 5. Figure 6 shows the wall-temperature variation
with time for stations 12 and 18 for a settling-chamber pressure of
220 pounds per square inch gage. Test runs were made for settling-chamber
pressures of 92, 142, 220, and 290 pounds per square inch gage. Excluding
the first 20 seconds, the pressures were maintained constant for each run.
The recorders were calibrated immediately before and after each run and
are accurate to $\pm 1^\circ$ F.

In figure 7 there are plotted for various times during the run the curves of wall temperature against longitudinal distance along the cylinder. These curves were used to determine the rate of change of the longitudinal conduction $k\dfrac{d^2T}{dx^2}$ along the cylinder. Test results were taken only for the length of the cylinder for which $k\dfrac{d^2T}{dx^2}$ was zero.

REDUCTION OF DATA

Short test runs in which wall-temperature—time histories are obtained give the essential data from which heat-transfer coefficients and recovery factors may be determined. The reduction of these data requires a method in which the stagnation temperature and, accordingly, the equilibrium temperature may vary in an arbitrary manner.

The Stanton number is calculated from

$$St = \frac{h}{\rho V C_p g} \qquad (1)$$

and the heat-transfer coefficient is calculated from

$$h = mc \, \frac{dT/dt}{T_w - T_{eq}} \qquad (2)$$

By definition, the recovery factor is

$$\eta_r = \frac{T_{eq} - T_\infty}{T_{stag} - T_\infty} \qquad (3)$$

The method of reducing the data is simply to select a recovery factor and from equation (3) obtain T_{eq}. Substitute this T_{eq} into equation (2) and obtain values of h for different heat flow rates. These values of h are then substituted into equation (1). The true values of T_{eq}, η_r, and St are obtained when the St is constant with time (different heat flow rates). Figure 8 shows the curves used in evaluating the Stanton number and the recovery factor for station 12 for a settling-chamber pressure of 220 pounds per square inch gage.

The values of specific heat and specific gravity of the sleeve material were taken from reference 2. Figure 9 gives the variation of the specific heat of the sleeve material with temperature. The values of viscosity and Prandtl number (0.71) for air were also taken from reference 2 and were based upon the inside surface temperature of the sleeve. The value of T_w chosen was at 120 seconds after starting. (This arbitrary choice of temperature can be made because the viscosity coefficient is practically a constant factor of the heat-conduction coefficient.)

ACCURACY

The basic data consist of temperature-time histories at each thermocouple location. The recorders were calibrated for synchronization immediately before and after each run and are accurate to $\pm 1^\circ$ F. The thermocouple wires are number-30-gage (0.010-inch diameter) copper-constantan wires. Conduction along the length for these wires is negligible. The wires are insulated except at the junction where intimate contact with the sleeve keeps thermal resistance to a minimum.

The sleeve is enclosed in a vacuum jacket to avoid free convection and, for the temperature range considered, radiation effects range up to 2 percent. The product of the mass per unit area and the specific heat of the sleeve material as used in equation (2) is accurate to ± 5 percent.

The value of dT/dt used in equation (2) is that of the actual thermocouple reading, whereas it should be the value associated with the average temperature in the thickness of the sleeve at each point. During the test runs, the inner-surface temperatures are lower than the average temperatures by approximately 1° to 1.5° at the beginning of the runs (40 seconds after starting) and become the same at the end of the runs (200 seconds). This effect results in the inner-surface temperature-time derivative being less than the average temperature-time derivative by approximately 1 percent. The computed slopes when integrated reproduce the original curves to within $\pm 0.5^\circ$ F.

The analysis of reference 3 was used to determine the effect of the sleeve diameter. This effect was computed to be less than 0.01 percent.

RESULTS AND DISCUSSION

Figure 7 shows the variation of wall temperature with longitudinal distance along the cylinder for a settling-chamber pressure of 220 pounds per square inch gage. Over the test range, the wall temperatures are constant with x. In the relation

$$h = \frac{mc \frac{dT}{dt}}{T_w - T_{eq}}$$

m and c are constant and dT/dt is constant because T_w is constant. Therefore, if there is to be a variation of h with Reynolds number or x, T_{eq} must vary with x. The value of T_{eq} obtained for the run with a chamber pressure of 220 pounds per square inch gage, evaluated at 120 seconds after starting, actually decreases approximately $2°$.

Figure 10 shows the variation of local Nusselt numbers with local Reynolds numbers. The x used in evaluating these numbers was based upon an x that was considered zero at the minimum. A single line faired through all the data points has a slope of approximately eight-tenths but, if lines are faired through the points for the individual runs, the slopes are slightly higher. It is reasonable to assume, however, that the higher stagnation pressures would produce earlier transition and hence the zero value of x would move upstream with increasing stagnation pressure. Hence, if it is assumed that the individual runs should merge into a continuous line (rather than a series of steps), x may be adjusted for $x = 0$ locations which would make all the runs coincident. This adjustment has been done in figure 11 by using values of x equal to zero at 2.00, 4.25, 7.25, and 10.00 inches ahead of the minimum for the runs with chamber pressures of 92, 142, 220, and 290 pounds per square inch gage, respectively. This systematic adjustment with pressure of the $x = 0$ location does not affect the value of a faired curve through all the data (figs. 10 and 11).

The Nusselt numbers were found to vary from 4,125 to 32,500 for the Reynolds number range of 5.6×10^6 to 6.5×10^7 (based on adjusted $x = 0$ locations). For comparison, the curves based upon the analyses of Van Driest (ref. 4) and Eber (ref. 5) are shown. In the Van Driest analysis, T_w/T_∞ was considered to be 3.0 (the average value of the test results). For comparison with these references, the data were computed by using the free-stream temperature to determine the density and the velocity. The wall temperature was used to determine the viscosity and Prandtl number. The two experimental values from V-2 data (ref. 6) are also determined in this manner.

The results of this paper are approximately 10 percent higher than the Van Driest analysis and approximately 27 percent higher than the Eber analysis. The V-2 experimental results coincide with the results of this paper.

Figure 12 shows the variation of local recovery factors with local Reynolds numbers. The variation is from 0.887 at 5.6×10^6 to 0.868 at 6.5×10^7. The results are compared with an extrapolated curve which

represents the fairing of the data of reference 7. The data of reference 7 are for Reynolds numbers below 6.75×10^6. The results of this report and those of reference 7 agree to within ± 0.5 percent. Also included for comparison are the curves for recovery factor equal to $Pr^{1/3}$ and $Pr^{1/2}$. The wall temperature was used to determine the Prandtl number.

CONCLUDING REMARKS

It can be concluded that the method of testing and reducing the data gives results that are in good agreement with established theoretical and experimental work. The reduction of the heat-transfer data requires adjusting the $x = 0$ locations (x is the longitudinal distance along sleeve) so that they are consistent when the Reynolds numbers are varied either by changing the pressure or the "x value" location. The variation of Nusselts number with Reynolds number before and after adjustment of the $x = 0$ locations are essentially the same.

The recovery-factor results are in good agreement with the extrapolated results of lower Reynolds number data.

Langley Aeronautical Laboratory,
    National Advisory Committee for Aeronautics,
        Langley Field, Va., June 24, 1954.

REFERENCES

1. Ferri, Antonio: Elements of Aerodynamics of Supersonic Flows. The Macmillan Co., 1949.

2. McAdams, William H.: Heat Transmission. Second ed. McGraw-Hill Book Co., Inc., 1942, p. 399.

3. Beckwith, Ivan E.: Heat Transfer and Skin Friction by an Integral Method in the Compressible Laminar Boundary Layer With a Streamwise Pressure Gradient. NACA TN 3005, 1953.

4. Van Driest, E. R.: The Turbulent Boundary Layer for Compressible Fluids on a Flat Plate With Heat Transfer. Rep. No. AL-997, North American Aviation, Inc., Jan. 27, 1950.

5. Eber, G. R.: Experimentelle Untersuchung der Bremstemperatur und des Wärmeüberganges an einfachen Körpern bei Überschallgeschwindigkeit. Archiv Nr. 66/57, Peenemunde, Nov. 21, 1941. (Translation GTR 22 by Engineering Dept., Chance Vought Aircraft, May 20, 1946.)

6. Fisher, W. W.: Supersonic Convective Heat Transfer Correlations From Skin-Temperature Measurements during Flights of V-2 Rockets No. 19 and No. 27. Rep. No. 55258, Gen. Elec. Co., July 1949.

7. Stalder, Jackson R., Rubesin, Morris W., and Tendeland, Thorval: A Determination of the Laminar-, Transitional-, and Turbulent-Boundary-Layer Temperature-Recovery Factors on a Flat Plate in Supersonic Flow. NACA TN 2077, 1950.

TABLE I

NOZZLE ORDINATES

x, in.	y, in.
0	3.532
.2	3.514
.4	3.4636
.6	3.3903
.8	3.3047
1.0	3.2156
1.6	2.9612
2.0	2.8036
2.6	2.5841
3.0	2.4482
3.6	2.2596
4.0	2.1436
4.6	1.9836
5.0	1.8856
5.6	1.7509
6.0	1.6687
6.6	1.5565
7.0	1.4888
8.0	1.3431
10.0	1.1490
12.320	1.0764
15.0	1.0484
20.0	.9934
25.0	.9384
29.0	.8944

-x, in.	y, in.
0	3.532
.2	3.527
.4	3.512
.6	3.482
.8	3.444
1.0	3.387
1.5	3.170
2.0	2.893
2.5	2.620
3.0	2.380
3.5	2.208
4.0	2.100
4.5	2.020
4.7	2.000
10.25	2.000

Figure 1.- Test arrangement.

Each wire wrapped and covered
Both wires form one lead from
each thermocouple.

Insulation (ceramic)

Sleeve (0.388 wall thick)
(steel)

Inner surface

0.060

Sleeve — $\frac{3}{32}$ O.D. x $\frac{1}{64}$ wall
(steel)

Tips of wires silver-
soldered together
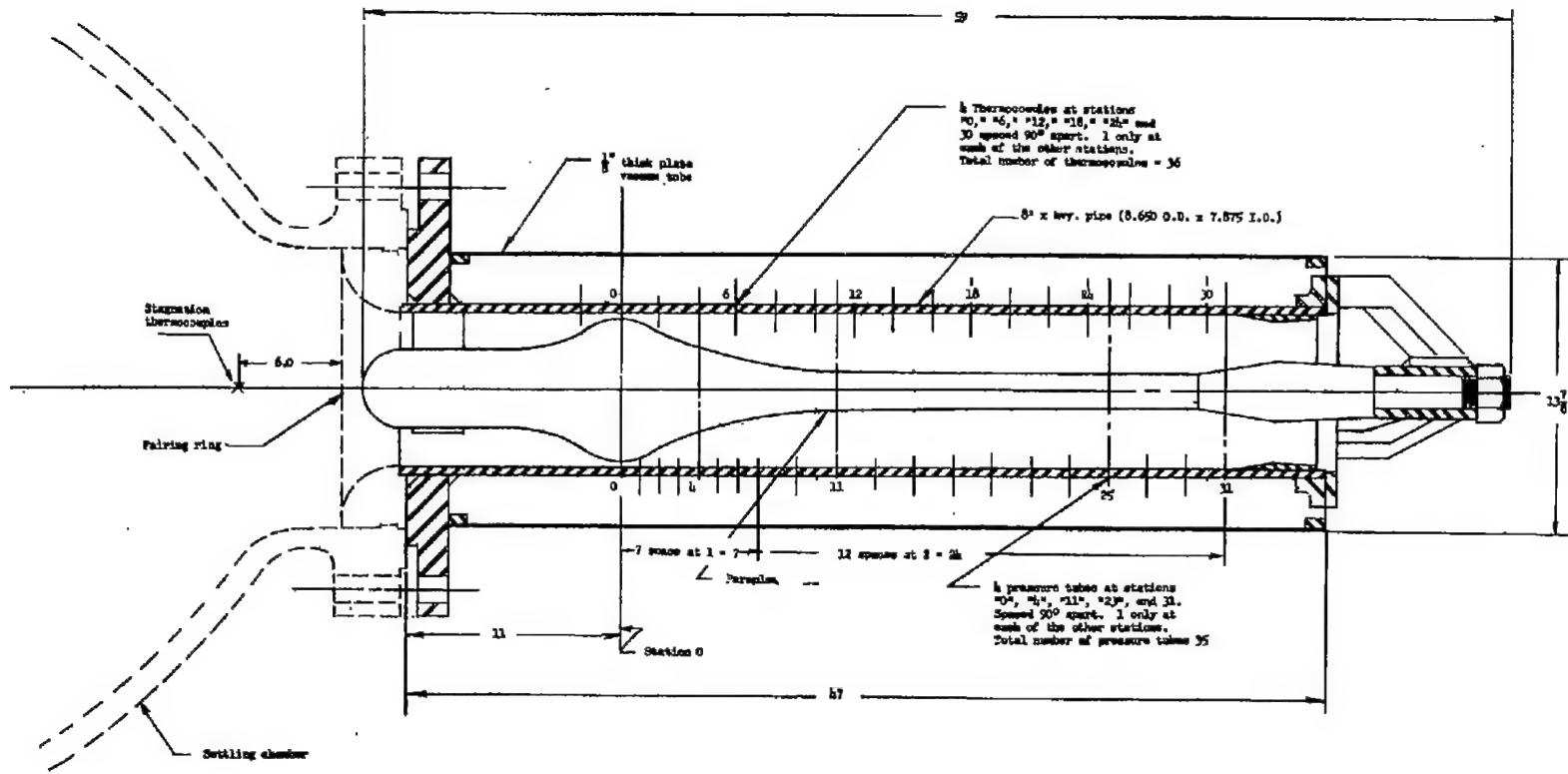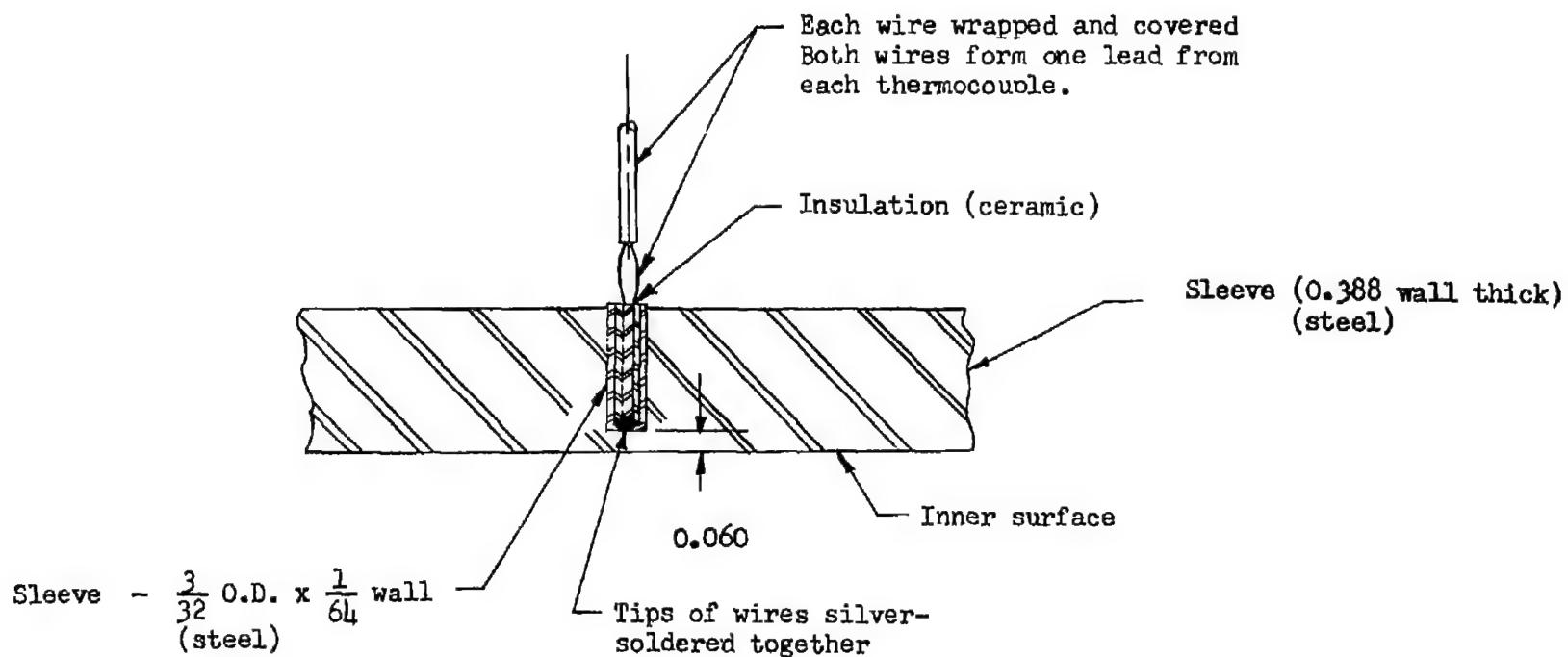
Figure 2.- Thermocouple installation.

No. 4/0 taper pin. Ream through
for 0.040" O.D. stainless steel
tubing.

Pressure tubes
(0.040 O.D. x 0.020
I.D. stainless steel)

Silver solder

Sleeve (0.388 wall thick)
(steel)

0.060

Inner surface
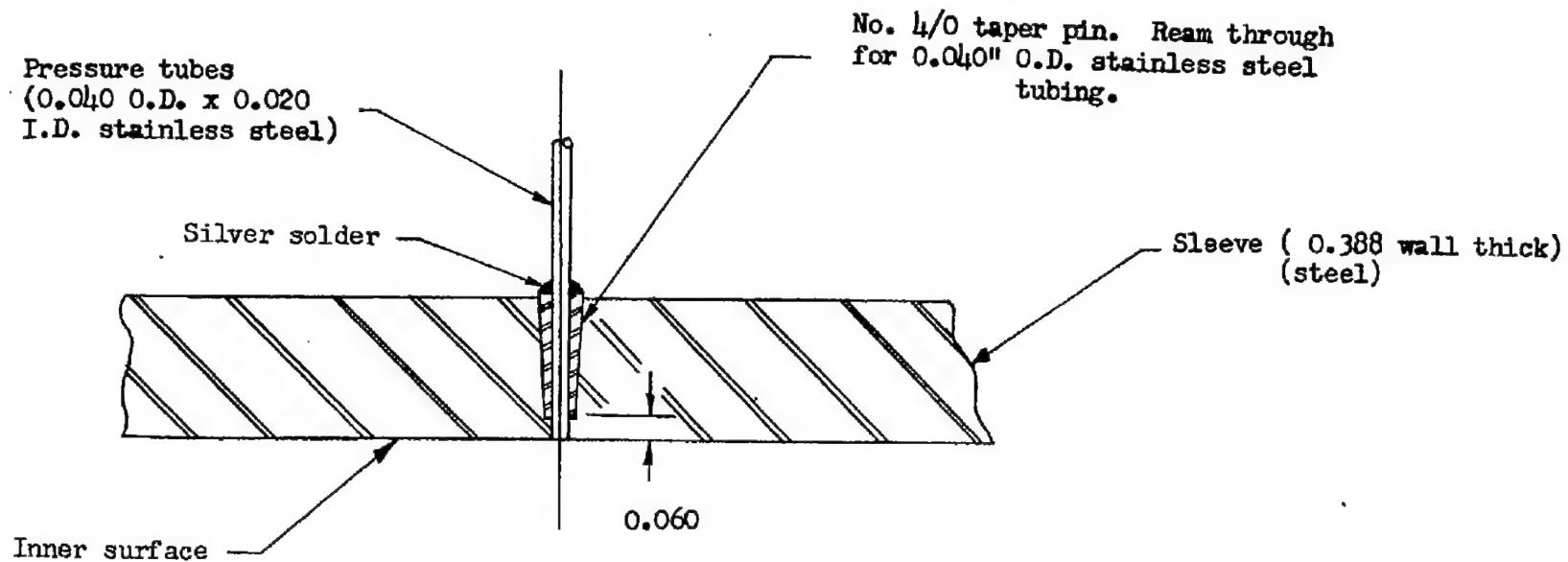
Figure 3.- Pressure tubes installation.
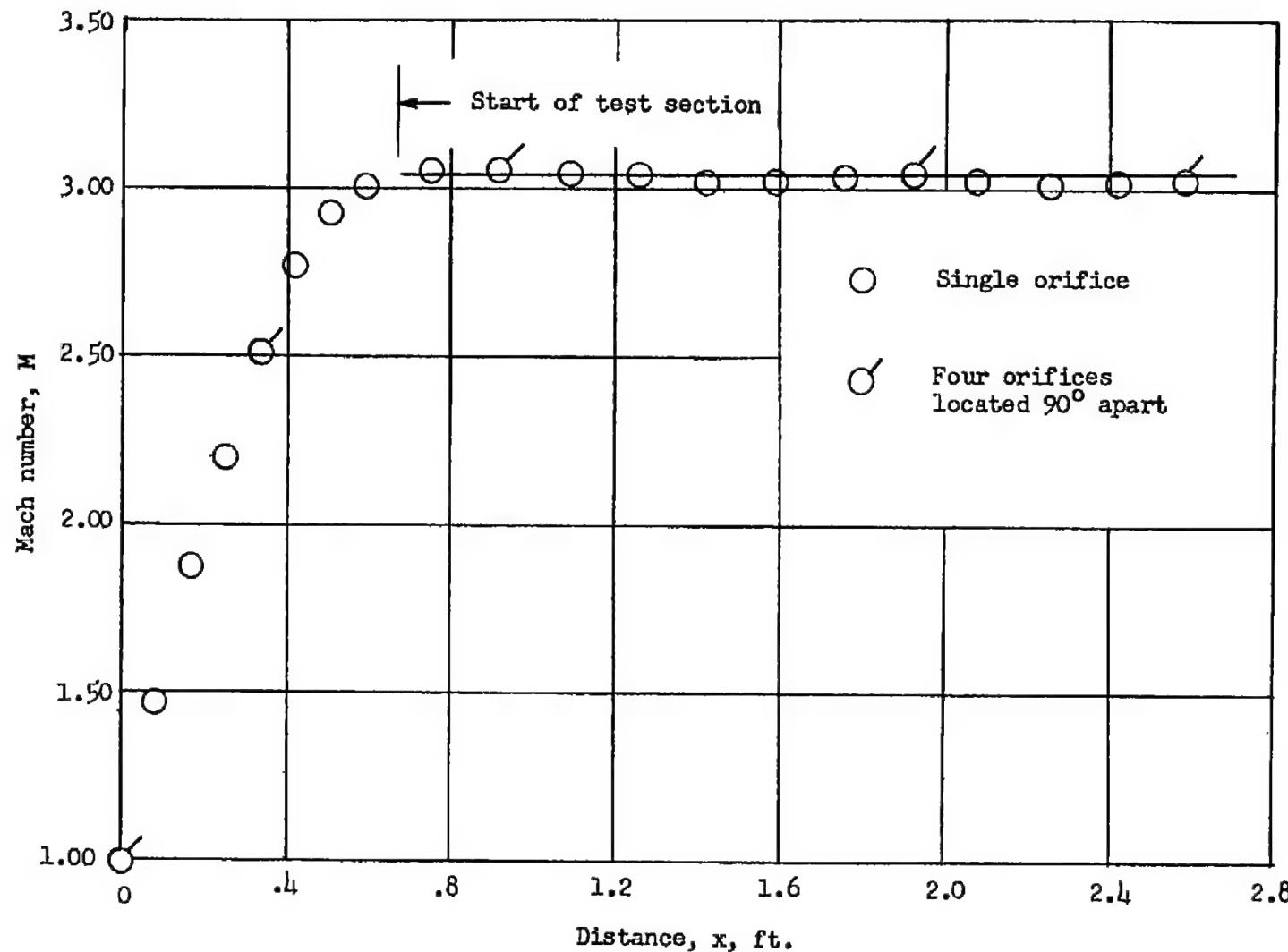
Figure 4.- Mach number distribution for settling chamber pressure of
220 pounds per square inch gage.
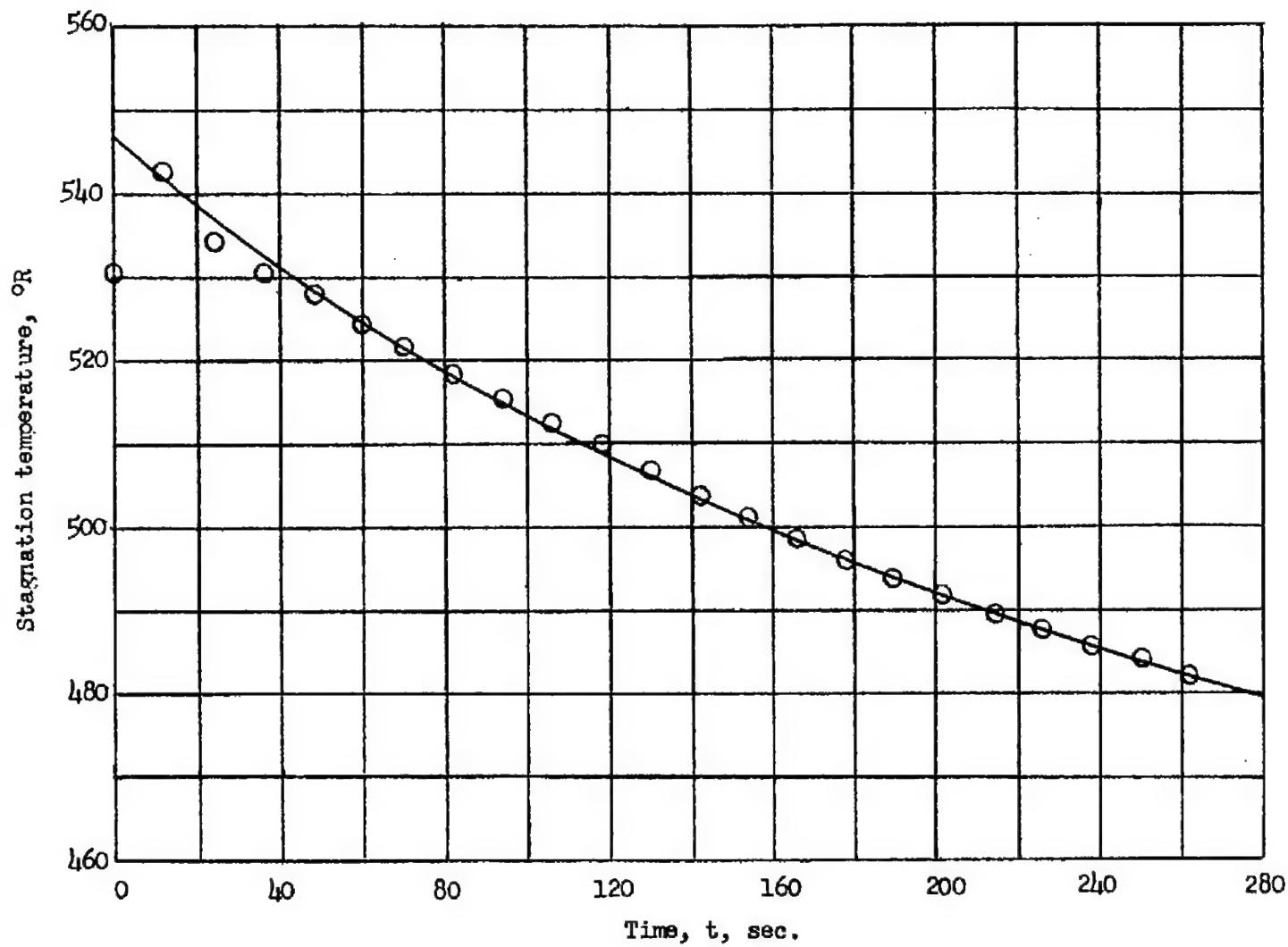
Figure 5.- Stagnation temperature variation with time for a settling chamber pressure of 220 pounds per square inch gage.
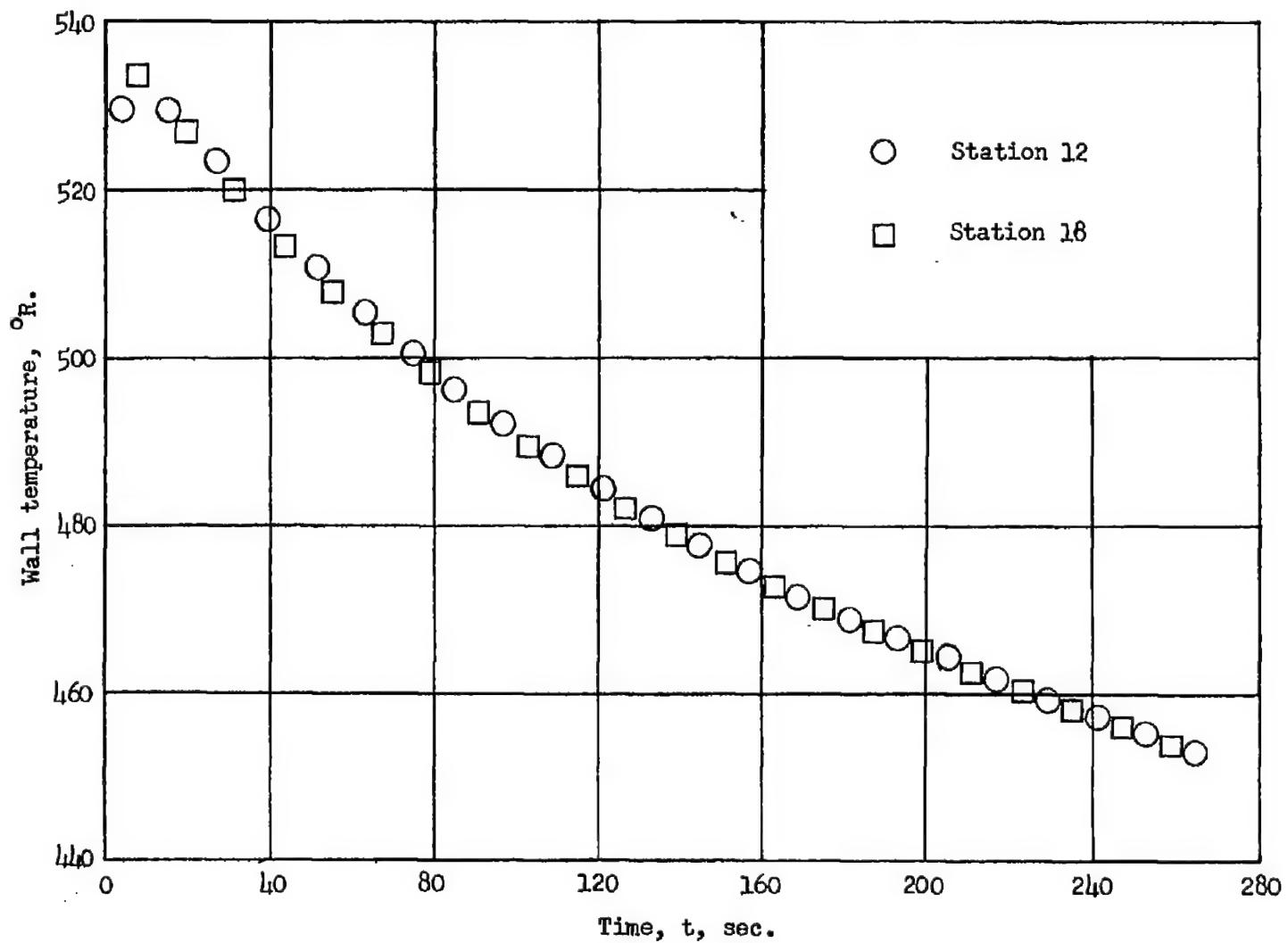
Figure 6.- Wall temperature variation with time for a settling chamber
pressure of 220 pounds per square inch gage.
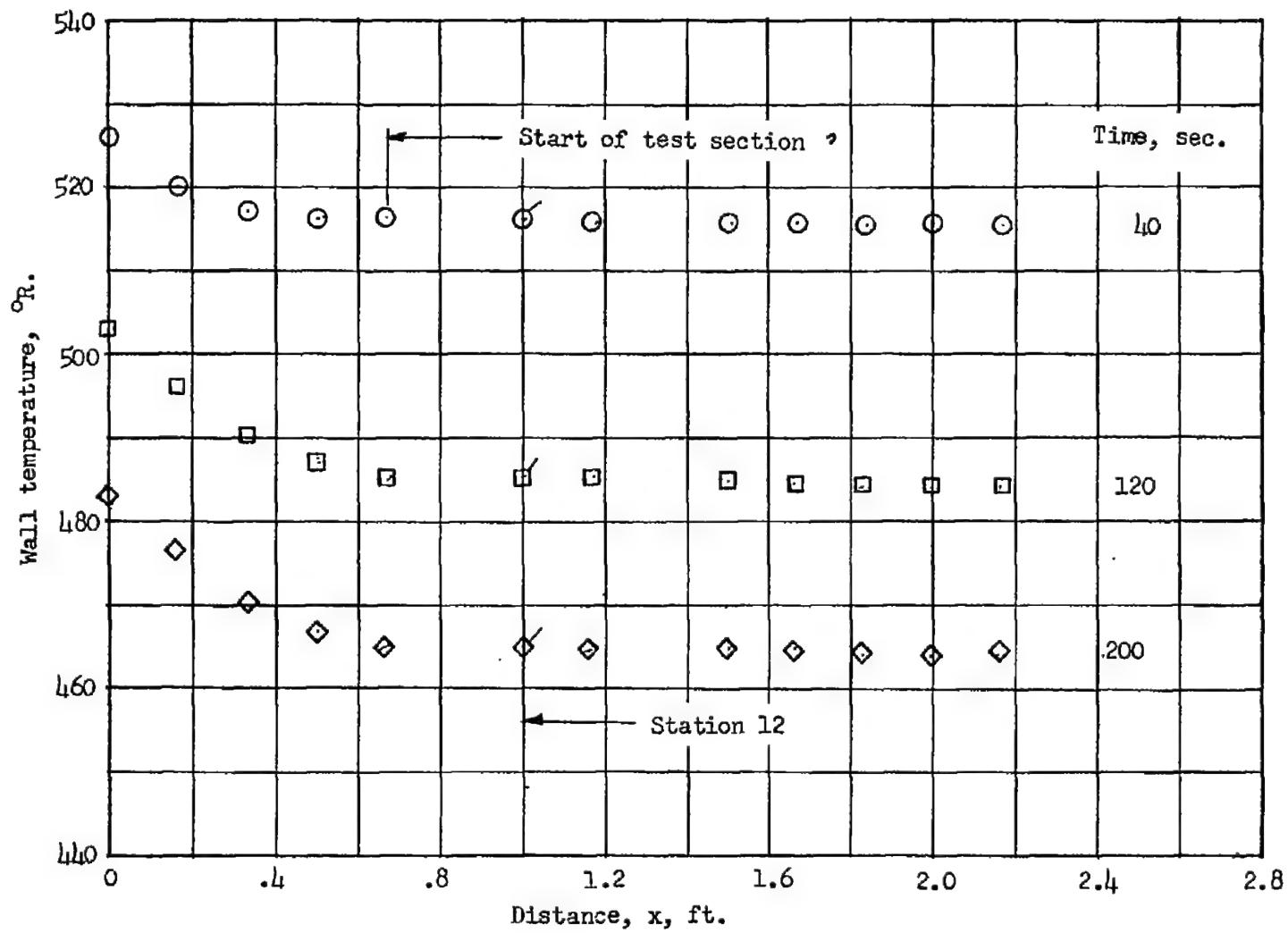
Figure 7.- Wall temperature variation with longitudinal distance for a settling chamber pressure of 220 pounds per square inch gage.
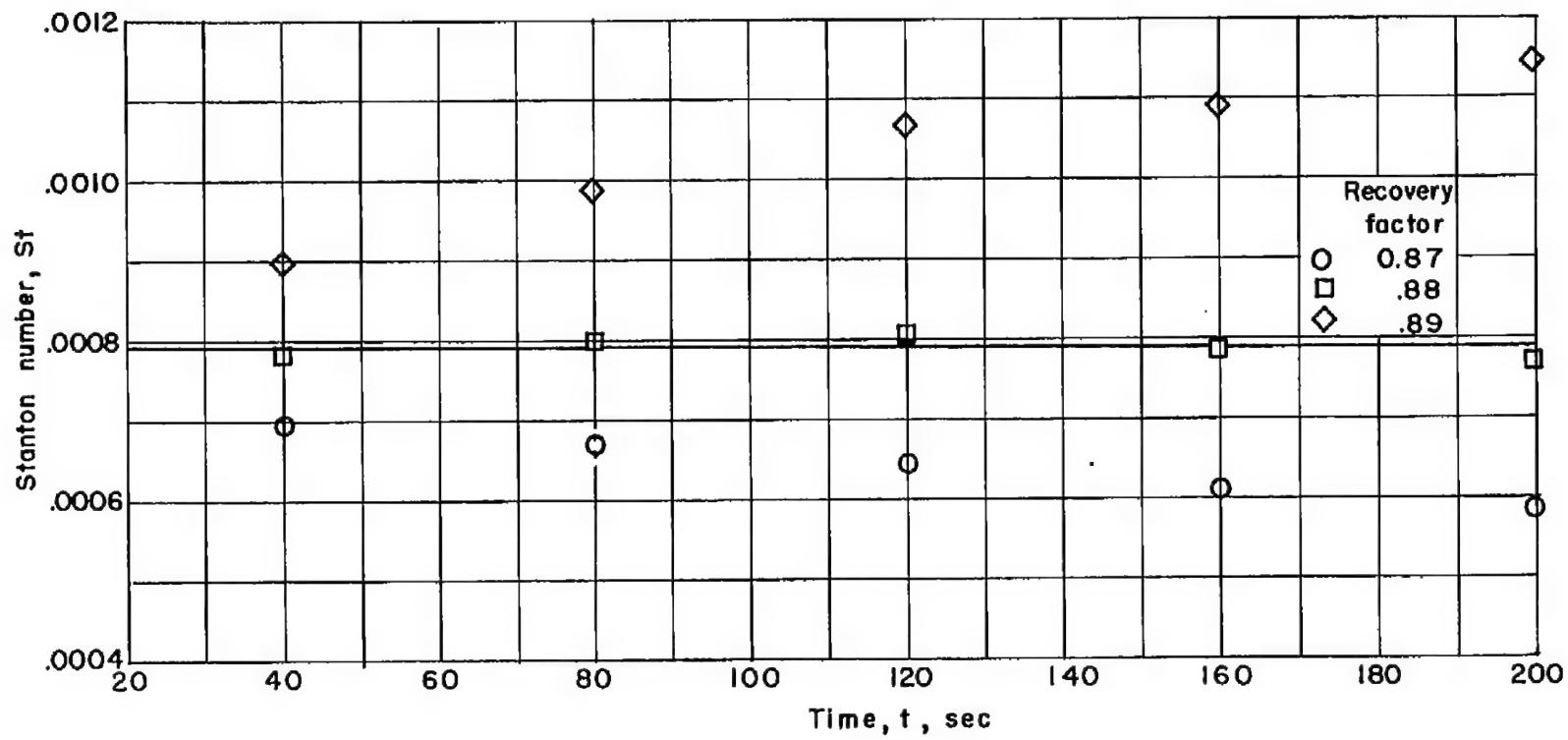
Figure 8.- Stanton number as a function of time and recovery factors for
    station 12 for a settling-chamber pressure of 220 pounds per square
    inch gage.
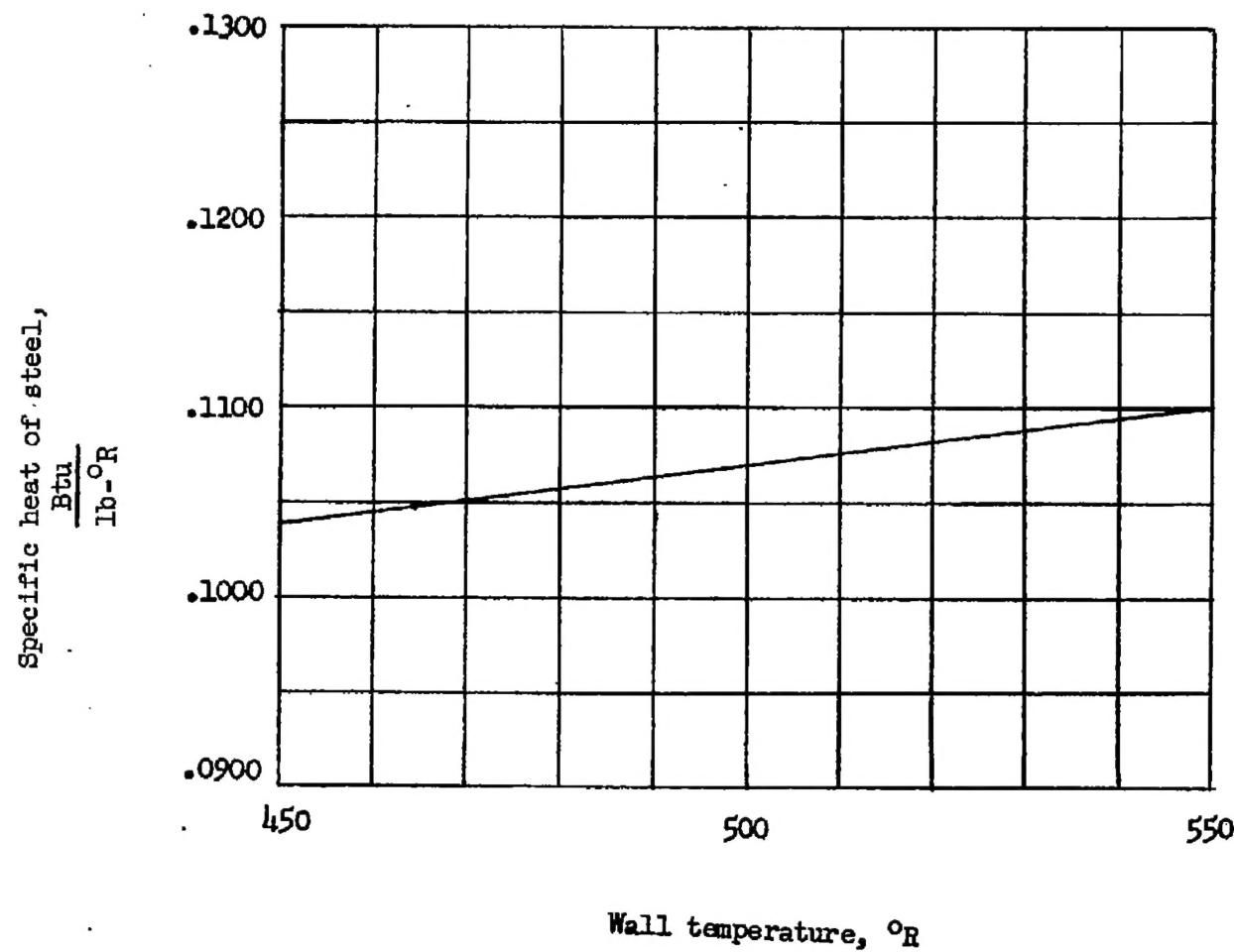
Figure 9.- Variation of specific heat of sleeve material with temperature.
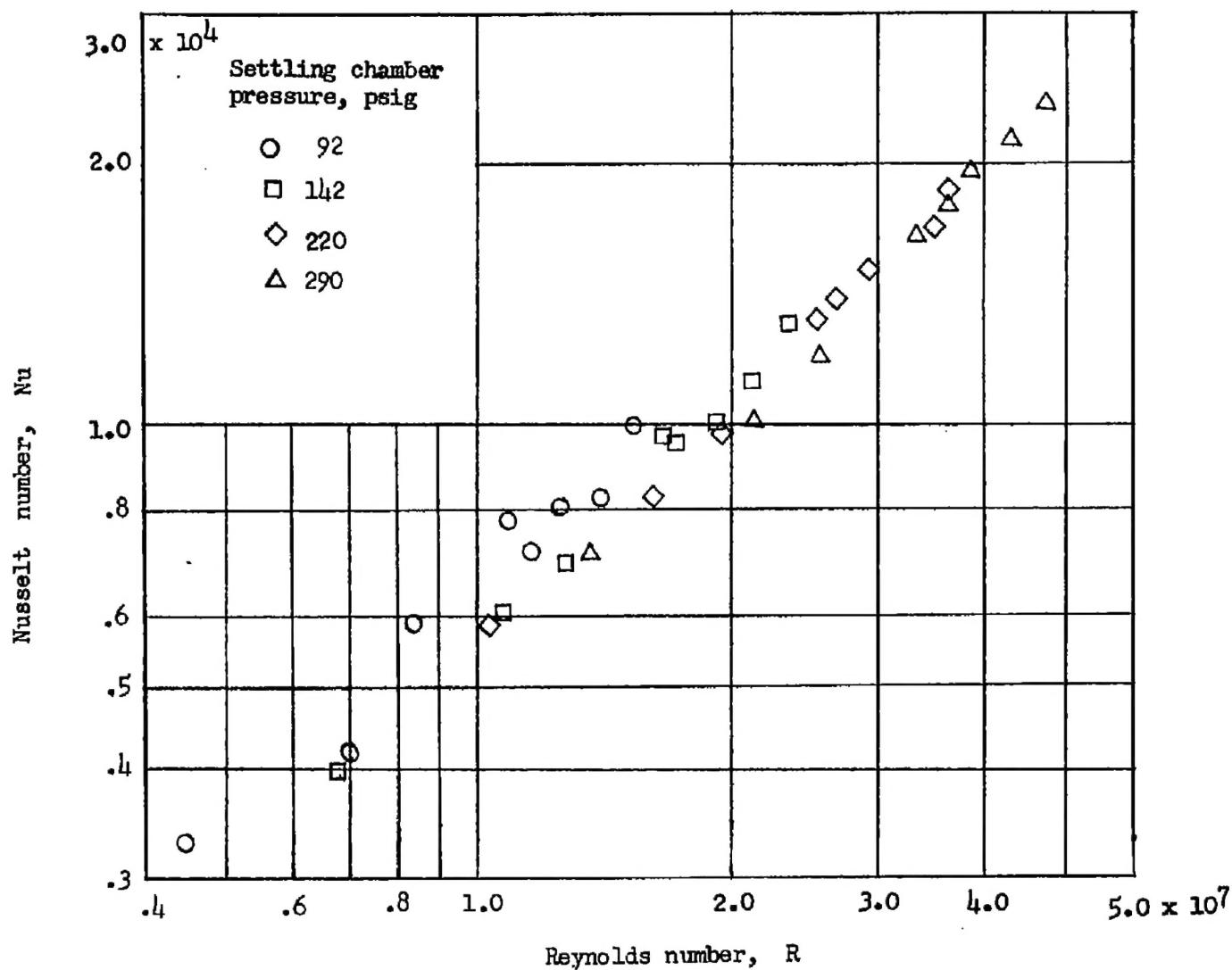
Figure 10.- Variation of local Nusselt number with local Reynolds number for $x = 0$ at station 0.
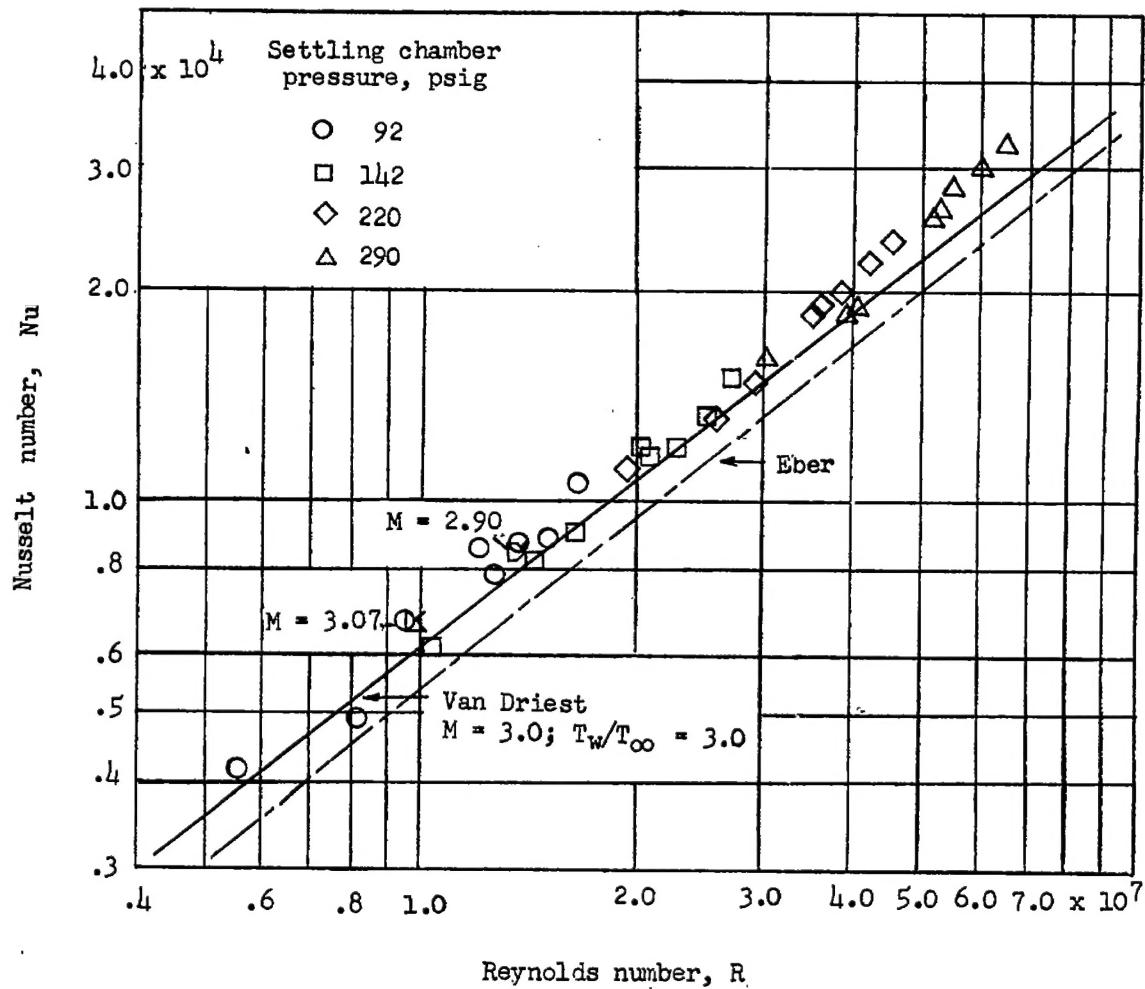
Figure 11.- Variation of local Nusselt number with local Reynolds number
for corrected .x = 0 locations. Viscosity and Prandtl number determined
for wall temperatures.
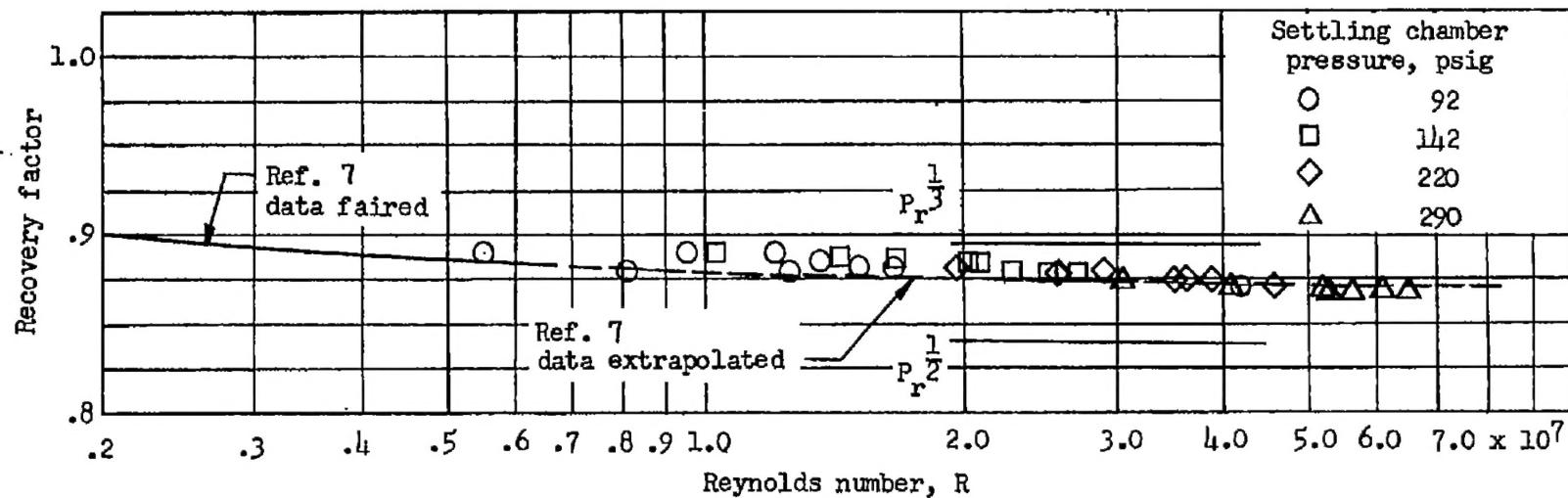
Figure 12.- Variation of local recovery factor with local Reynolds number for corrected .x = 0 locations. Viscosity determined for wall temperatures.